Effects of biodeterioration on the mechanical properties of concrete

Jorge Fernando Marquez-Peñaranda, Mauricio Sanchez-Silva, Johana Husserl, Emilio Bastidas-Arteaga

Please cite this paper as:
Marquez-Peñaranda JF, Sanchez-Silva M, Husserl J, Bastidas-Arteaga E (2016). Effects of biodeterioration on the mechanical properties of concrete. Materials and Structures. In press. http://doi.org/10.1617/s11527-015-0774-4

Effects of biodeterioration on the mechanical properties of concrete

J. F. Marquez-Peñaranda[a,b], M. Sanchez-Silva[a*], J. Husserl[a] and E. Bastidas-Arteaga[b].

[a] Department of Civil and Environmental Engineering, Universidad de Los Andes, Carrera 1 Este No. 19A-40, Edificio Mario Laserna, Piso 6, Bogotá, Colombia
[b] LUNAM Université, Université de Nantes-Ecole Centrale Nantes, GeM, Institute for Research in Civil and Mechanical Engineering/Sea and Littoral Research Institute, CNRS UMR 6183/FR 3473, 2, rue de la Houssinière BP 99208, 44322 Nantes Cedex 3, France.

ABSTRACT

Concrete biodeterioration in sewers and structures subjected to environments rich in hydrogen sulfide has been related to the activity of sulfur oxidizing bacteria (SOB). In previous studies, the growth of SOB in sulfur rich environments has been mainly linked to weight loss of concrete structures. In our work we have investigated, in addition to the weight loss, the variations in porosity and compressive strength that result from the metabolism of SOB. The main objective of the paper is to explore, under controlled conditions, the effect of biodegradation of non-submerged samples, on physical properties and mechanical performance. Towards this aim, cement mortar samples inoculated with pure cultures of *A. thiooxidans*, *H. neapolitanus*, and a consortium containing both strains, were exposed to an H2S-rich environment. Changes in physical properties, including weight and porosity, and compressive strength were measured as a function of time over 300 days. The greatest reduction of weight and compressive strength was observed in samples inoculated with the consortium (7% and 52%, respectively). The largest variation in porosity was observed in samples inoculated with *A. thiooxidans* (27%). These results were finally used to propose preliminary biodeterioration models.

Keywords:

Concrete, biodeterioration, porosity, compressive strength, weight loss, sulfur oxidizing bacteria

1 INTRODUCTION

Life-cycle analysis and modeling of infrastructure requires the understanding of its performance over time, which depends highly on the characterization of material degradation [1–4]. Although phenomena such as aging, fatigue and corrosion are known to be important agents for concrete degradation, it has been noted that in aggressive environments the action of living organisms also affects critical infrastructure. These problems have been reported in, for example, oil pipelines [5], underground structures, sewage systems [6], and offshore structures [7,8]. Biodeterioration affects mainly concrete durability increasing maintenance costs [9,10], and reducing the capacity of structural members in the long term.

Biodeterioration is usually overlooked in most structural analyses because its kinematics is very slow and then it remains undetected or neglected during the structural lifetime. Furthermore, biodeterioration itself is not a cause of failure, but it plays an important role in reinforced concrete degradation by accelerating other damaging processes such as chloride ingress and carbonation, and consequently corrosion propagation and loss of capacity [1,11]. In concrete structures, biodeterioration affects the concrete matrix by increasing porosity, reducing strength and the cross-section area of components, and promoting crack growth. In

* Corresponding author: M. Sánchez-Silva. Address: Carrera 1 Este No. 19A-40, Edificio Mario Laserna, Piso 6, Bogotá, Colombia; Phone: (+571) 3324312; Fax: (+571) 3324313 email: msanchez@uniandes.edu.co

particular, it is well known that microbially induced degradation is a main concern in sewage collection systems. Due to anoxic conditions commonly found in sewage, sulfate in wastewater is used as an electron acceptor and sulfide is produced. At low pH, hydrogen sulfide gas volatilizes and rises to the tops of sewer pipes where aerobic microbial communities grow in biofilms [12,13]. Sulfur oxidizing bacteria (SOB) living in these biofilms use hydrogen sulfide or reduce sulfur compounds as electron donors and oxygen from air as an electron acceptor. The oxidation process generates sulfate or sulfuric acid [13,14] that reacts with the calcium hydroxide of the cement matrix forming calcium sulfate. Calcium sulfate reacts with calcium aluminate hydrate to form ettringite, which is an expansive material [15], resulting in concrete degradation observed as weight loss or the detriment of mechanical properties [16].

Many bacteria are capable of oxidizing sulfur yet only a handful of species are commonly found on corroded concrete surfaces in sewers. The microbial autotrophic species capable of inorganic sulfur oxidation *Acidithiobacillus thiooxidans, Halothiobacillus neapolitanus, Starkeya novella,* and *Thiomonas intermedia* have been widely associated with concrete biodeterioration. The most aggressive strains with respect to biodeterioration are all members of the phylum proteobacteria [17–23]. SOB are all capable of growing on reduced sulfur compounds as electron donors. Substrates used by these species include hydrogen sulfide or metal sulfides such as pyrite, sulfur, polysulfides, sulfite, and thiosulfate [24]. The ecology of the sulfur oxidizing microbial communities is highly dependent on the pH of the concrete matrix [19,25]. After casting, the pH of concrete is about 12, which inhibits sulfur-oxidizing bacteria development. In sewer pipes, however, carbonation and exposure to hydrogen sulfide reduce concrete pH to a point at which neutrophilic sulfur oxidizing bacteria can grow and produce sulfuric acid, which also lowers the pH even further to a point at which acidophiles thrive. Sulfur-oxidizing bacteria start to accumulate once the pH reaches about 8. The optimum pH for the development of these bacteria vary between 5.02–8.41 and 0.1–5.86 for *H. neapolitanus* and *A. thiooxidans*, respectively [2]. As a result, *H. neapolitanus* can be found on concrete at the beginning of the biocolonization when the pH is still high. But acid production by this and other organisms can lower pH to values at which the most acidophilic species, *A. thiooxidans*, thrive.

Several studies focused on the weight loss as an indicator of biodeterioration activity [2,18,19,26–29]. They report a wide range of weight loss observations (even for similar environmental conditions) ranging from negligible weight loss after 126 days of exposure [26] to total weight loss (100%) after 350 days [27]. The heterogeneity of the cementitious mortars and concrete, the variability of the environmental conditions, and the interactions and dynamics of the microorganisms involved in sulfur oxidation are only some of the aspects adding complexity to the description and quantification of the biodeterioration process.

Biodeterioration could also affect other physical and mechanical properties of concrete. During concrete biodeterioration process, a layer of high porosity is produced by acid attack. This high porosity layer leads to greater permeability and diffusion within the inner matrix of the material [30]. On the other hand, compressive strength decreases for larger porosities in concrete and mortar specimens [31–34]. Consequently, the compressive strength of concrete components could be affected by biodeterioration and must therefore be modeled as a time-variant property throughout the structural lifetime [35]. Although porosity and strength variations due to biodeterioration are paramount for structure condition assessment, to the authors´ knowledge, nowadays there are no studies that include these parameters.

Within this context, the objectives of this study are:

- to evaluate biodeterioration effects on weight loss, porosity and compressive strength under a controlled environment,
- to propose preliminary models to assess the effects of biodeterioration on these concrete properties, and
- to analyze the relationships between these three properties.

The novel contribution of this study is the assessment of biodegradation of non-submerged samples, on physical properties (porosity and weight) and mechanical performance (i.e., compressive strength). Results from this study would contribute to a better description of concrete biogenic corrosion processes, and consequently, to provide specific quantitative information on concrete biodeterioration effects. This information is needed to improve the assessment of biodeterioration effects on concrete durability over time.

Section 2 presents the design of the experiment and the basic considerations for deriving the preliminary models. The results of the experiments are provided and discussed in section 3. Section 3 also presents the proposed models for the assessment of biodeterioration effects. The final part of section 3 focuses on studying the relationships between the biodeterioration effects on weight loss, porosity and strength of concrete.

2 MATERIALS AND METHODS

In our work we exposed mortar samples (inoculated with pure strains and non-inoculated) to H_2S-rich environments and measured their physical and mechanical changes during 300 days. In the next subsections a description of physical, biological and chemical conditioning of samples is presented. Also the scope and limitations of the proposed models are stated.

2.1 Mortar sample preparation

Portland cement mortar 13 mm x 13 mm x 10 mm samples with water-to-cement ratio w/c=0.485 were cast into a plastic container without a mold release agent. Casting was made by compacting two successive layers with a plastic rammer after 30 seconds of vibration with a pneumatic-motor-table. ASTM C778-06 standard graded natural river sand and Portland cement type I were used to prepare the samples. Cement paste-sand mix was blended using a five-pound mixer (Hamilton Beach Commercial) with a cement-to-sand ratio of 1:2.75. Casting molds containing fresh samples were wrapped with stretch film and stored at 20°C for 24 hours. Demolded samples were subjected to 90% relative humidity (RH) curing for 30 days inside closed plastic boxes. Cured samples were oven dried at 110°C for 24 hours and then subjected to an "ordinary atmospheric" period for 60 days at 20±2°C and 60±10% RH.

2.2 Inoculum, growth conditions, and verification of microbial purity

Hallothiobacillus neapolitanus NCIMB 8454 and ASOM *Acidithiobacillus thiooxidans* NCIMB 9112 (ATCC8085) were purchased from American Type Culture Collection – (ATCC) (Virginia, USA). Pure cultures were grown in DSMZ (Deutsche Sammlung von Mikroorganismen und Zellkulturen) 68 *Thiobacillus neapolitanus* agar/liquid medium or DSMZ 35 *Thiobacillus thiooxidans* agar/liquid medium, as recommended by supplier. Prior to inoculating mortar samples, bacterial cells were grown in liquid media to an optical density (OD) 600 of 1.0. Cultures were centrifuged (4°C, 13000 rpm, 15 min) to separate cells from growth medium and were triple washed with mineral medium containing no source of sulfur. Washed cells suspended in mineral medium (without sulfur) were used to inoculate mortar samples. Oven-dried mortar samples were soaked in cell suspensions of *A. thiooxidans*, *H. neapolitanus*, or a consortium of both. Before inoculation and throughout the experiment (300 days), purity and presence of cultures was verified morphologically after growth in Luria Bertani (LB) agar. No changes were observed in bacterial morphology of cultured plates from samples collected at different ages.

2.3 Experimental setup

Surface alkalinity of the mortar samples was reduced through carbonation (20% CO_2, 15 days, 60±10% RH). Surface pH of all samples was reduced from around 12 to less than 9 (verified with phenolphthalein test) [36–39]. Five groups, composed of 76 samples each one, were wrapped in foil and oven dried at 110°C for 24 hours (for sterilization). No bacterial growth was observed when some concrete oven-dried samples were "stamped" on LB agar. One group of 76 samples was inoculated with *H. neapolitanus* (H.n.), a second group was inoculated with *A. thiooxidans* (A.t.), and the third group was inoculated with a consortium (Cons.) composed by both bacteria. The fourth group was composed of abiotic samples exposed to the same environment of the biotic samples (i.e. H_2S+CO_2). The remaining group was used as control in which abiotic samples were exposed to a sterile environment at the same temperature (30±1°C) and relative humidity (62±5) of the other four groups (Table 1). For simplicity in the results of this paper the chemical exposure condition (fourth group) will be referred solely as H_2S.

All groups of samples were placed in individual 5 cm x 18 cm x 18 cm hermetic plastic containers (Fig. 1). During the first 150 days of the experiment, sulfide was supplied to each container every 3 days to a H_2S concentration of about 100 ppmv. During the last 150 days, feeding was conducted on a daily basis, reaching

the same concentration of hydrogen sulfide. Containers were maintained with 0.3±0.1% CO_2. Distilled water, HCl, $Na_2S•9H_2O$ and $NaHCO_3$ were mixed and placed in the bottom of each container to achieve the required concentrations of H_2S and CO_2. The device used for the exposure of the samples in each test had an 8-mm height liquid layer, a plastic bearing structure and a plastic net over which samples were placed distanced 25 mm from the water surface. Mixing of distilled water, sodium sulfide, sodium bicarbonate and hydrochloric acid was achieved by means of slight movements of three small crystal balls after closing the container. Container sealing was verified by reading outside H_2S concentration within a sealed 30cm x 40cm x 60cm incubator after four hours of gas accumulation. Containers showed no leaks at the beginning of the experiment but at the end of the experiment showed almost 1 ppmv H_2S after four hours of accumulation. Portable Gas Analyzer BioGas CDM (LANDTEC ®) and Portable Gas Analyzer RKI GX2009 (RKI Instruments ®) were used to measure H_2S, CO_2 and O_2 levels.

A central element of the study is the variation of H_2S concentration over time (Fig. 2). Addition of hydrogen sulfide and carbon dioxide resulted in the production of the gases in the environment that rapidly decreased over time. H_2S decrease (at a rate of 12±4 ppmv/h) was about constant throughout the experiment. H_2S was available to microorganisms for only about 8 hours after addition of the chemicals to the liquid underneath the mortar samples. The rapid decrease of hydrogen sulfide concentration in the headspace suggests that there is a high sorption capacity of the concrete samples. It is likely that at low H_2S headspace concentrations, biogenic effects became more important than chemical sorption [40]. Fig. 3 shows the sulfur availability *Sa(t)* through the time. The sulfur availability is the accumulated amount of sulfur applied (mg) with respect to the exposed area (cm^2) of the samples at each age. Exposed-area-to-weight ratio of mortar samples was of 2.91±0.01 cm^2/g.

2.4 Assessment of biodeterioration effects on physical and mechanical properties

Compressive strength, weight loss and porosity of samples were measured over 300 days of exposure to bacterial attack. These measurements were made after 0, 60, 120, 195, 240 and 300 days of exposure. Additional measurements for weight loss and compressive strength were taken at days 30, 90, 150 and 270. Samples were extracted from containers following a uniform-random selection sampling method. Once extracted, moist samples were weighed and later oven dried (110°C for 24 hours). The humid weight and dry weight of the samples were measured using a precision scale (Ohaus Adventurer Pro Analítica AV264). To ensure correct weight measurements, prior to weighing, extracted samples were subjected to a passive wash in which they were submerged in distilled water for one hour and shaken for 30 seconds every 20 minutes before being placed into the oven. Nine weight measurements were taken and averaged for each sample.

Porosity measurements in triplicate were taken using mercury intrusion data from an AutoPore IV 9500 porosimeter (Micromertics Instrument Corporation). Pores in solids can be classified according to their size as micropores, mesopores or macropores. In general it is accepted that adsorbed water can be found in micropores, condensed water in mesopores and bulk water in macropores [41]. In civil engineering applications, micropores are most commonly accepted to have widths between 0.5 and 10 nm, mesopores between 10 and 5000 nm, and macropores larger than 5000 nm [34]. This study used this standard (micropores being 0-10 nm, mesopores being 10-5000 nm and macropores being larger than 5000 nm).

Compressive strength was measured in triplicate using a 500 kg load cell hydraulic press (ELE International Digital Tritest). Records of load versus deformation at a deformation speed of 0.10 mm/min were obtained for samples at each stage of the experiment. A pre-load equivalent to 1.0–1.5 MPa was applied five minutes prior to the start of the test to ensure uniform pressure on the upper and lower surfaces of each sample. Upper and lower surfaces were leveled prior to testing using rubber pieces. Compressive strength values were scaled so that results were comparable to the results of standard 5-cm-side-cube compressive load tests [42].

2.5 Considerations for modeling biodeterioration effects

This study is based on an experiment in which the concrete alkalinity was dropped down using carbonation prior to inoculation and exposure of samples. For this reason the experiment start time actually represents the stage of active biodeterioration once the concrete pH has been reduced and the concrete surface has been conditioned for a long time. The length of the first stage (biodeterioration immunity) could be estimated by

using carbonation models until a given pH level [48,49]. Therefore, the preliminary biodeterioration models developed in this section are only applicable after the biodeterioration immunity stage has been overcome. To generalize the results, they have been normalized with respect to the cumulated sulfur availability (Fig. 3). Since the results were obtained from measurements taken during 300 days of exposure (or $Sa(t) \leq 20 mg/cm^2$), the assessment of biodeterioration effects after this time (or sulfur availability) should be carried out with care. Other limitations of the preliminary models are summarized as follows:

- This study has solely considered one type of cement mortar. The models provide a first attempt for evaluating biodeterioration effects but the results could vary for different mortar/concrete compositions.
- The experiment was controlled to avoid the presence of other bacteria and therefore the models are only valid for this kind of exposure. Different results could be observed for other bacteria.

2.5.1 Normalization of results

This normalization aims at generalizing the results when samples are exposed to different environments of those used in this experiment. All the biodeterioration effects (weight, porosity and strength changes) can be expressed as a function of the sulfur availability $Sa(t)$:

$$Sa(t) = 0.2628e^{0.0146t} \quad (1)$$

where $Sa(t)$ is expressed in mg of elemental sulfur per cm^2 of exposed surface of mortar existing at time t (days) (Fig. 3). Although control specimens were not exposed to biodeterioration, for comparison purposes, results of these specimens were expressed in function of sulfur availability by considering the $Sa(t)$ values at different measurement times.

2.5.2 Models and assessment of model parameters

By studying mean trends of biodeterioration effects, it is possible to identify two deterioration stages. In the first one, biodeterioration effects are not significant and therefore they are neglected for modeling. In the second one, three curve fittings were proven: linear and second-degree polynomial and logarithmic equations. Solver tool by Microsoft Excel was used to identify the model parameters that minimize the mean square error in each case. In all cases the best fit was achieved by using logarithmic fittings.

By taking into account the amount of data considered for each measure (section 2.4), it was also possible to evaluate the error of the proposed models. This error is modeled as a normal random value and their mean and standard deviation are computed from:

$$\mu_{ME,y}(Sa(t)) = \frac{1}{n_m}\sum_{i=1}^{n_m}\left[\hat{y}_i(Sa(t)) - y_m(Sa(t))\right] \approx 0 \quad (2)$$

$$\sigma_{ME,y}(Sa(t)) = \sqrt{\frac{1}{n_m - 1}\sum_{i=1}^{n_m}\left[\left(\hat{y}_i(Sa(t)) - y_m(Sa(t))\right) - \mu_{ME,y}(Sa(t))\right]^2} \quad (3)$$

where $\mu_{ME,y}(Sa(t))$ and $\sigma_{ME,y}(Sa(t))$ are the mean and standard deviation of the error of the model respectively. The error of the model was computed as the difference between the i^{th} measured value $\hat{y}_i(Sa(t))$ and the value provided by the model $y_m(Sa(t))$ for a given $Sa(t)$. Here y represents the studied deterioration parameter: weight, strength or porosity variation

3 RESULTS AND DISCUSSION

Qualitative observations related to color and texture changes were recorded at each sampling time. Samples showed stains of different colors during the experiment: gray, green, bronze, and white shades appeared successively upon samples surfaces during the experiment. White crystals (which are supposed to be ettringite crystals) were visible after 90 days of exposure in biotic samples. Such crystals were observed only after 210 days over samples subjected to chemical exposure. This section reports measured changes in weight, strength and porosity produced by biodeterioration.

3.1 Weight variation

Weight variation was computed for each sample at the correspondent age as:

$$\Delta w(t) = \frac{w(t) - w_i}{w_i} * 100 \qquad (4)$$

where $\Delta w(t)$ is the weight variation (%), *w(t)* is the dry weight (mg) measured at time *t* and w_i is the initial dry weight (mg) measured at time t=0. As mentioned in section 2.5.1 all the results are expressed as a function of sulfur availability for generalization purposes. Fig. 4 and 5 indicate that by the end of exposure (i.e., $Sa(t)\approx 21$ mg/cm^2), samples inoculated with the consortium showed a total weight loss of 6.8±1.4%. Samples inoculated separately with *A. thiooxidans* and *H. neapolitanus* lost 4.6±1.4% and 2.4±0.5% of their initial weight, respectively. In contrast, weight gains of 1.0±0.8% and 0.5±0.6% were observed in abiotic samples exposed to H_2S and samples belonging to control, respectively. The abiotic samples exposed to hydrogen sulfide likely gained weight as a result of the accumulation of precipitated sulfur. The small weight variation in the control samples is within the expected error of the experimental measurement technique. Fig. 4 and 5 include all measurements (from 6 to 9 measures) by exposure time. The greatest data variability was observed in samples inoculated with *Acidithiobacillus thiooxidans* (Fig. 5).

Overall results indicate greater weight loss after feeding frequency was changed from once every three days to every day (day 150 or $Sa(t)\approx 2.7$ mg/cm^2 in Fig. 2, 4 and 5). Larger weight changes started after $Sa(t)\approx 1.8$ mg/cm^2 (120 days) in all biotic samples. Lower weight losses during the first three months of the experiment resulted from the time required for superficial conditioning (pH drop, biofilm formation, roughness adaptation) and bacterial lag phase. After this span the acidophilic bacteria (pure and within the consortium) seemed to be capable of growing faster and acidifying the concrete surface leading to greater weight loss. The effect of the neutrophilic bacteria on the weight of the samples was less pronounced. The lower effects of *H. neapolitanus* than *A. thiooxidans* on the weight of the samples could be a result of differences in growth rates, selectivity of the reduced sulfur metabolites available, accumulation of toxic byproducts, and other metabolic differences in general.

Fig. 5 shows the mean values of the weight variation depending on the sulfur availability *Sa(t)* within the surrounding environment. Negligible weight variation is associated to *Sa(t)* smaller than a threshold value Sa_{th}=1 mg/cm^2. This limit corresponds to the accumulated sulfur applied during the first 90 days of exposure (Fig. 3). It is also noted that the mean weight change follows a logarithmic trend after this value. Table 3 summarizes the best fit equations for the weight variation once $Sa(t) \geq 1$ mg/cm^2. It is assumed that there is no weight variation ($\Delta w = 0$) if $Sa(t) < 1$ mg/cm^2.

Fig. 5 indicates that the dispersion of data from biotic samples increases with the exposure time. The largest standard deviation increase was associated to the presence of *A. thiooxidans* alone or within the consortium. Standard deviation for control samples and those exposed to H_2S was constant during the exposure time. Standard deviation of control samples can be associated to uncertainties related to material (intrinsic uncertainty) and the test. Standard deviation of samples exposed to H_2S can be related to uncertainties coming from the exposure without biological activity. By comparing uncertainties at the end of the exposure, it is concluded that biodeterioration multiplies by about two or three the initial uncertainties (intrinsic, test and H_2S exposure). Table 3 provides the adjusted expressions for the standard deviation for all experimental conditions. Fig. 5 compares the proposed models and measured data for weight change. It is observed that in most part of experimental results are within the 95% confidence interval.

3.2 Porosity variation

3.2.1 Changes in porosity at micro, meso and macro levels

When measuring porosity, mercury intrusion expressed in ml/g is used to compute the pores volume existing inside a sample. Fig. 6 shows the cumulative intrusion curves for all samples in three different exposure times (0, 120, and 300 days). At the end of the experiment, control samples showed the lowest total mercury intrusion (0.087 ml/g) resulting from its natural trend of the mortar to decrease its porosity with time. Final porosity was linked to total mercury intrusions of 0.114, 0.151, and 0.133 ml/g for samples inoculated with *H. neapolitanus*, *A. thiooxidans* and the consortium, respectively. Abiotic samples exposed to hydrogen sulfide resulted in a total mercury intrusion of 0.128 ml/g. The reduced porosity variation in samples inoculated with *H. neapolitanus* is consistent with their minor weight losses. The major porosity increase was observed for pores between 0.05 nm and 10 mm in samples inoculated with *A. thiooxidans*. Interestingly, those show a pore volume increase for pore sizes around 1um (1000nm) which is the average length of the *A. thiooxidans* bacillus. Samples inoculated with the consortium and abiotic samples exposed to H_2S showed an increase in pores between 5000 and 10000 nm suggesting the formation of new capillary connections.

3.2.2 Effects in total porosity

Porosity variation was computed for each sample at the correspondent age as:

$$\Delta\phi(t) = \phi(t) - \phi_i \qquad (5)$$

where $\Delta\phi(t)$ is the porosity variation (%), $\phi(t)$ is the porosity (%) measured in each sample at time t and ϕ_i is the initial porosity (%) measured in control sample at time $t=0$.

Total porosity of any material can be computed as the sum of isolated pores volume existing inside the solid structures plus open (connected) pores volume existing amid those solid structures [43]. In this work only open porosity was measured and for simplicity it is called “porosity”. Average porosity (in volume) and its distribution were determined from three measurements for each type of sample. Initial porosity (prior to exposure, at time t=0) of all samples was about 19% with a coefficient of variation COV=0.12. Initial porosity and its COV were computed using six samples randomly chosen from the population of available samples. Fig. 4 and 7 summarize the evolution of porosity measured during the exposure time. After 300 days, the porosity of biotic samples increased significantly. Final porosities up to 27%, 25% and 22% were measured in samples inoculated with *A. thiooxidans*, the consortium and *H. neapolitanus*, respectively. Control samples reduced their porosity down to 18% while abiotic samples exposed to H_2S increased it up to 24%. Error bars were drawn using minimum and maximum values from 3 measures at each exposure time. Similar variability at each age was observed in all samples.

Table 2 describes the initial and final porosities in pore ranges for the studied cases. The volume of micropores (0–10 nm) showed a visible change only for samples inoculated with the consortium. This fact suggests that biodeterioration produced by the consortium was able to affect the concrete microstructure. From a comparison with the control samples, it is evident that the volume of mesopores increased from 13.4% to 21.7% in samples inoculated with *A. thiooxidans* while the volume of macropores increased from 3.2% to 8.3% in samples inoculated with the consortium. According to this, *A. thiooxidans* could be the responsible for largest variations in mesopores while the consortium for those related to macropores. Also it has been reported that macropores increase is associated to compressive strength decrease [31,34]. This fact could explain the greater strength drop observed in samples inoculated with the consortium. Also changes in macropores and mesopores could be related to changes in pores connectivity affecting the permeability and durability of the material.

Fig. 7 presents the porosity variation as a function of the sulfur availability. The porosity increase was estimated as 7%, 6% and 4% for samples inoculated with *A. thiooxidans*, the consortium and those abiotic exposed to H_2S respectively. Minor porosity increase of about 2% was related to the samples inoculated with *H. neapolitanus* while a porosity reduction of 2% was associated to the control samples. Fig. 7 lets infer two

trends of porosity changes depending on the sulfur availability. A rapid porosity increase for all exposed samples is observed for sulfur availability values *Sa(t)* between 1 and 5 mg/cm^2. In general larger changes in porosity are observed in acidic conditions (*A. thiooxidans,* consortium and chemical exposure) and almost negligible porosity variations are linked to neutral conditions (*H. neapolitanus*). Negligible porosity variation is associated to *Sa(t)* smaller than a threshold value Sa_{th}=1 mg/cm^2. This limit corresponds to the accumulated sulfur applied during the first 90 days of exposure (Fig. 3). It is also noted that the porosity change follows a logarithmic trend after this value. Table 3 summarizes the best fit equations for the porosity variation for *Sa(t)*≥1 mg/cm^2. It is assumed that there is no porosity variation ($\Delta\phi$=0) if *Sa(t)*<1 mg/cm2. Due to the existence of only three measurements at each age, the standard deviation for each experimental condition has been computed as a unique value using the totality of data. Fig. 7 compares the proposed models and measured data for porosity change. It is evident that practically all experimental results are within the 95% confidence interval.

3.3 Compressive strength variation

For simplicity, the compressive strength is referred solely as "strength" in the next sections. Typical compressive breaking of all tested samples showed cracks parallel to load axis revealing pressure-application uniformity. Average initial strength was 30 MPa (COV=0.03) and 33 MPa (COV=0.02) for non-carbonated and carbonated 90-day-old samples, respectively. Abiotic carbonated samples (control) were used as the reference to compute the relative strength (Fig. 4 and 8). Strength variation was computed for each sample at the correspondent age by:

$$\Delta s(t) = \frac{s(t) - s_i}{s_i} * 100 \qquad (6)$$

where $\Delta s(t)$ is the strength variation (%), *s(t)* is the strength (MPa) measured in each exposed sample at time *t* and s_i is the initial strength (MPa) measured in the control sample at time *t=0*. After 300 days of exposure, samples inoculated with *H. neapolitanus*, *A. thiooxidans* and abiotic samples subjected to H_2S showed a strength loss equivalent approximately to 28% of their initial value. Control samples did not show important strength variations. Samples inoculated with the consortium lost more than a half (52%) of their initial strength (Fig. 4 and 8). Furthermore, the most important strength loss was observed between days 60 and 90 for the same samples. These results confirm that the interaction among the microorganisms in consortium is a predominant factor for biodeterioration. By comparing strengths of samples inoculated with pure strains and those abiotic samples coming from chemical exposure, it is observed that the strength loss is caused mainly by the chemical effect of hydrogen sulfide over the mortar samples. Consequently, biogenic deterioration from pure strains seems not to contribute in an important manner to relative strength changes. Error bars were drawn using minimum and maximum values from three samples per exposure time. The largest data variability at each age was observed in samples inoculated with *Acidithiobacillus thiooxidans* (Fig. 8).

Fig. 8 shows the relative strength variation with respect to the sulfur availability. Negligible strength variation is associated to *Sa(t)* smaller than a threshold value Sa_{th}=1 mg/cm^2. This limit corresponds to the accumulated sulfur applied during the first 90 days of exposure (Fig. 3). It is also noted that the strength change follows a logarithmic trend after this value. Table 3 summarizes the best fit equations for the strength variation for *Sa(t)*≥1 mg/cm^2. It is assumed that there is no strength variation (Δs=0) if *Sa(t)*<1 mg/cm2. In general the strength losses caused by the activity of the consortium doubled those produced by others conditions under the same sulfur availability. It is evident the larger influence of acidophilic bacteria (pure or within a consortium) in the strength variation. Fig. 8 compares the proposed models and measured data for porosity change. It is noted that most of experimental results are within the 95% confidence interval.

3.4 Relationships between weight, strength and porosity variations in biodeteriorated samples

3.4.1 Strength – weight variations relations

While Fig. 5 shows negligible weight losses during the first three months, Fig. 8 indicates an important strength loss in the same lapse. This trend is reversed during the remaining months of the experiment. This fact seems to indicate that the major intensity of biogenic activity is related to larger weight loss and smaller strength variation. A rapid weight loss is linked to the overcoming of the bacterial lag phase while the bacterial growth seems to be associated to a buffer effect in the strength deterioration. This averment could be explained by virtue of a positive effect in the compressive strength coming from clogging and deposition of biodeterioration byproducts in the inner mortar matrix.

Fig. 9 (left side) depicts the strength losses to weight losses relations modeled for biodeteriorated samples. Two zones well delimited can be identified in which straight lines built from data showed good correlation for all biotic samples. The initial part of the graph (left edge) covers strength losses up to about a half of the total loss. Low weight losses between 0.3 and 0.6% are associated to large strength losses from 11% to 28%. Minor strength losses are related to a wider weight losses range (0.6% to 7%). These findings suggest that the most important strength deterioration could occur even when weight or thickness losses are not visible yet.

3.4.2 Strength – porosity variations relations

The trend of the relationship between strength and porosity of samples exposed to biodeterioration is similar to that reported in literature for cement pastes, mortars and concretes in no biodeteriorated samples [32–34,44–47]. In general, strength decreases when porosity increases. However, the relationship between strength and porosity changes depends on the experimental conditions (Fig. 10). A similar compressive-strength-to-porosity slope was observed for samples inoculated with *A. thiooxidans* and those coming from chemical exposure. In contrast, a sharper slope was obtained for samples inoculated with *H. neapolitanus* and the consortium. These results suggest that concrete microstructure changes due to biodeterioration are affected differently depending on the type of bacteria involved in the process. Indeed the neutrophilic bacteria seem to have clogged the porous structure in a major proportion than acidophilic bacteria did.

Porosity gain to weight loss relation observed in biodeteriorated samples is modeled in Fig. 9 (right side). Best fit was achieved using straight lines for all biotic samples. Similarly to as exposed in section 3.4.1, strength losses up to about a half of the total loss are linked to small porosity gain. Low porosity augments increases of 0.6 and 1.9% are associated to large strength losses from 11% to 28%. Strength losses of the same order are associated to a wider porosity gains range (1.9% to 7.2%).

4 CONCLUSIONS

Samples inoculated with the consortium showed the major signs of biodeterioration with larger weight loss, important porosity changes and minor final strength. Also pure acidophilic bacteria were able to produce a high biodeterioration mainly depicted by weight loss and porosity augment. Conversely samples inoculated with pure neutrophilic bacteria had a similar behavior to the abiotic samples subjected to H_2S. These results suggest that the ecology of the system influences in an important manner the biodeterioration effects.

In this study the samples were subjected only to a gaseous environment with low H_2S concentrations. These observations may indicate a major relative biodeterioration in here than in previous researches in which samples have been partially submerged. This effect could be explained by the fact that our samples had a high exposed-surface-to-mass-ratio. On the other hand, porosity and strength tests were undertaken in non-modified samples (tested as they were cast) ensuring more realistic results than when samples have been manipulated previously (cut and brushed as it has been made in other studies).

Proposed models for weight, porosity and strength variation show a good correspondence with data. A key factor in modeling is related to the sulfur availability threshold of about 1 mg/cm^2 from which all the biodeterioration effects are evident. In all cases the best fit was obtained using logarithmic equations.

Further work to be done on the experimental quantification of biodeterioration effects is recommended related to:

- the design of laboratory protocols and experimental setups capable of quantifying the bacterial growth over the exposed surfaces samples using advanced microbiological tools,
- the implementation of superficial pH measurements to describe in a comprehensive manner the material acidification process, and,
- the evaluation of the biodeterioration synergy involving variables related to the ecology of microorganisms, the influence of their symbiosis, mutualism and competition relations.

Acknowledgements

The authors want to acknowledge the financial support of the Universidad Francisco de Paula Santander (Colombia). The fourth author acknowledges the support of the 'Pays de la Loire' region (France) for funding the Coselmar project (Compréhension des Socio-Ecosystèmes Littoraux et Marins pour l'Amélioration de la Valorisation des Ressources Marines, la Prévention et la Gestion des Risques) http://www.coselmar.fr.

REFERENCES

[1] Bastidas-Arteaga E, Sánchez-Silva M, Chateauneuf A, Ribas Silva M. Coupled reliability model of biodeterioration, chloride ingress and cracking for reinforced concrete structures. Struct. Saf. 2008;30:110–129.

[2] Bielefeldt A, Gutierrez-Padilla MGD, Ovtchinnikov S, Silverstein J, Hernandez M. Bacterial Kinetics of Sulfur Oxidizing Bacteria and Their Biodeterioration Rates of Concrete Sewer Pipe Samples. J. Environ. Eng. 2010;136:731–738.

[3] Wei S, Jiang Z, Liu H, Zhou D, Sanchez-silva M. Microbiologically induced deterioration of concrete - A Review. 2013;1007:1001–1007.

[4] Bertron A. Understanding interactions between cementitious materials and microorganisms: a key to sustainable and safe concrete structures in various contexts. Mater. Struct. 2014;47:1787–1806.

[5] Videla HA. Manual of Biocorrosion. CRC Press, 1996.

[6] Cho K, Mori T. A newly isolated fungus participates in the corrosion of concrete sewer pipes. Water Sci. Technol. 1995;31:263–271.

[7] Melchers RE, Jeffrey RJ. Probabilistic models for steel corrosion loss and pitting of marine infrastructure. Reliab. Eng. Syst. Saf. 2008;93:423–432.

[8] Melchers RE. The effect of corrosion on the structural reliability of steel offshore structures. Corros. Sci. 2005;47:2391–2410.

[9] Kumar R, Gardoni P, Sanchez-Silva M. Effect of cumulative seismic damage and corrosion on the life-cycle cost of reinforced concrete bridges. Earthq. Eng. Struct. Dyn. 2009;38:887–905.

[10] Sanchez-Silva M, Klutke G-A, Rosowsky D V. Life-cycle performance of structures subject to multiple deterioration mechanisms. Struct. Saf. 2011;33:206–217.

[11] Bastidas-Arteaga E, Sánchez-Silva M, Chateauneuf A. Structural reliability of RC structures subject to biodeterioration, corrosion and concrete cracking, in: J. Kanda, T. Takada, H. Furuta (Eds.), 10th Int. Conf. Appl. Stat. Probab. Civ. Eng., Tokyo:Japan: 2007: pp. 183–190.

[12] Sawyer CN, McCarty PL, Parkin GF. Chemistry for Environmental Enginnering and Science. McGraw Hill, 2003.

[13] Dopson M, Johnson DB. Biodiversity, metabolism and applications of acidophilic sulfur-metabolizing microorganisms. Environ. Microbiol. 2012;14:2620–31.

[14] Madigan M, Martinko JM, Parker J. Brock biology of microorganisms. 2000.

[15] O'Connell M, McNally C, Richardson MG. Biochemical attack on concrete in wastewater applications: A state of the art review. Cem. Concr. Compos. 2010;32:479–485.

[16] Nnadi EO, Lizarazo-Marriaga J. Acid Corrosion of Plain and Reinforced Concrete Sewage Systems. J. Mater. Civ. Eng. 2013;25:1353–1356.

[17] Wei S, Sanchez M, Trejo D, Gillis C. Microbial mediated deterioration of reinforced concrete structures. Int. Biodeterior. Biodegradation 2010;64:748–754.

[18] Sand W. Importance of Hydrogen Sulfide , Thiosulfate , and Methylmercaptan for Growth of Thiobacilli during Simulation of Concrete Corrosion. Appl. Environ. Microbiol. 1987;53:1645–1648.

[19] Okabe S, Odagiri M, Ito T, Satoh H. Succession of sulfur-oxidizing bacteria in the microbial community on corroding concrete in sewer systems. Appl. Environ. Microbiol. 2007;73:971–80.

[20] Islander RL, Devinny JS, Mansfeld F, Adam P, Hong S. Microbial ecology of crown corrosion in sewers. J. Environ. Eng. 1991;117:751–770.

[21] Hernandez M, Marchand EA, Roberts D, Peccia J. In situ assessment of active Thiobacillus species in corroding concrete sewers using fluorescent RNA probes. Int. Biodeterior. Biodegradation 2002;49:271–276.

[22] Giannantonio DJ, Kurth JC, Kurtis KE, Sobecky P a. Molecular characterizations of microbial communities fouling painted and unpainted concrete structures. Int. Biodeterior. Biodegradation 2009;63:30–40.

[23] Coleman RN, Gaudet ID. Thiobacillus Neopolitanus implicated in the degradation of concrete tanks used for potable water storage. Water Res. 1993;27:413–418.

[24] Friedrich CG, Bardischewsky F, Rother D, Quentmeier A, Fischer J. Prokaryotic sulfur oxidation. Curr. Opin. Microbiol. 2005;8:253–9.

[25] Hudon E, Mirza S, Frigon D. Biodeterioration of concrete sewer pipes: State of the art and research needs. J. Pipeline Syst. … 2011;42–52.

[26] Lors C, Chehade MH, Damidot D. pH variations during growth of Acidithiobacillus thiooxidans in buffered media designed for an assay to evaluate concrete biodeterioration. Int. Biodeterior. Biodegradation 2009;63:880–883.

[27] Ehrich BS, Helard L, Letourneux R, Willocq J, Bock E. Biogenic and chemical sulfuric acid corrosion of mortars. J. Mater. Civ. Eng. 1999;340–344.

[28] Monteny J, De Belie N, Vincke E, Verstraete W, Taerwe L. Chemical and microbiological tests to simulate sulfuric acid corrosion of polymer-modified concrete. Cem. Concr. Res. 2001;31:1359–1365.

[29] Herisson J, van Hullebusch ED, Moletta-Denat M, Taquet P, Chaussadent T. Toward an accelerated biodeterioration test to understand the behavior of Portland and calcium aluminate cementitious materials in sewer networks. Int. Biodeterior. Biodegradation 2013;84:236–243.

[30] Beddoe RE, Dorner HW. Modelling acid attack on concrete: Part I. The essential mechanisms. Cem. Concr. Res. 2005;35:2333–2339.

[31] Ba M, Qian C, Guo X, Han X. Effects of steam curing on strength and porous structure of concrete with low water/binder ratio. Constr. Build. Mater. 2011;25:123–128.

[32] Chen X, Wu S, Zhou J. Influence of porosity on compressive and tensile strength of cement mortar. Constr. Build. Mater. 2013;40:869–874.

[33] Chindaprasirt P, Rukzon S. Strength, porosity and corrosion resistance of ternary blend Portland cement, rice husk ash and fly ash mortar. Constr. Build. Mater. 2008;22:1601–1606.

[34] Kumar R, Bhattacharjee B. Porosity , pore size distribution and in situ strength of concrete. Cem. Concr. Res. 2003;33:155–164.

[35] Mahmoodian M, Alani AM. Multi-Failure Mode Assessment of Buried Concrete Pipes Subjected to Time-Dependent Deterioration , Using System Reliability Analysis. J Fail. Anal.and Preven. 2013;13:634–642.

[36] Giannantonio DJ, Kurth JC, Kurtis KE, Sobecky P a. Effects of concrete properties and nutrients on fungal colonization and fouling. Int. Biodeterior. Biodegradation 2009;63:252–259.

[37] Wiktor V, De Leo F, Urzì C, Guyonnet R, Grosseau P, Garcia-Diaz E. Accelerated laboratory test to study fungal biodeterioration of cementitious matrix. Int. Biodeterior. Biodegradation 2009;63:1061–1065.

[38] Thiery M. Modélisation de la carbonatation atmosphérique des matériaux cimentaires Prise en compte des effets cinétiques et des modifications microstructurales et hydriques, École Nationale Des Ponts Et Chussees, 2005.

[39] Herisson J. Biodétérioration des matériaux cimentaires dans les ouvrages d'assainissement – Etude comparative du ciment d'aluminate de calcium et du ciment Portland, Université Paris-Est, 2012.

[40] Jensen HS, Nielsen a H, Lens PNL, Hvitved-Jacobsen T, Vollertsen J. Hydrogen sulphide removal from corroding concrete: comparison between surface removal rates and biomass activity. Environ. Technol. 2009;30:1291–6.

[41] Setzer MJ. Action of frost and deicing chemicals - basic phenomena and testing, in: Free. Durab. Concr., 1997: pp. 3–23.

[42] American Society for Testing Materials. ASTM C109/C109M − 12. Standard Test Method for Compressive Strength of Hydraulic Cement Mortars (Using 2-in . or [50-mm] Cube Specimens). 2012.

[43] Rouquerol J, Avnir D, Fairbridge CW, Everett DH, Haynes JH, Pernicone N, et al. Recommendations for the characterization of porous solids. Pure Appl. Chem. 1994;66:1739–1758.

[44] Kolias S. Investigation of the possibility of estimating concrete strength by porosity measurements. Mater. Struct. 1994;27:265–272.

[45] Lam L, Wong YL, Poon CS. Degree of hydration and gel / space ratio of high-volume fly ash / cement systems. 2000;30:

[46] Zhao H, Xiao Q, Huang D, Zhang S. Influence of Pore Structure on Compressive Strength of Cement Mortar. Hindawi Publ. Corp. 2014;2014:1–12.

[47] Pichler B, Hellmich C, Eberhardsteiner J, Wasserbauer J, Termkhajornkit P, Barbarulo R, et al. Strength Evolution of Hydrating Cement Pastes: the Counteracting Effects of Capillary Porosity and Unhydrated Clinker Reinforcements, in: Poromechanics V ASCE, 2013: pp. 1837–1846.

[48] Duracrete. Modelling of Degradation, DuraCrete - Probabilistic Performance based Durability Design of Concrete Structures, EU - Brite EuRam III, Contract BRPR-CT95-0132, Project BE95-1347/R4-5. 1998.

[49] De Larrard T, Bastidas-Arteaga E, Duprat F, Schoefs F. Effects of climate variations and global warming on the durability of RC structures subjected to carbonation. Civ. Eng. Environ. Syst. 2014;31:153–164.

List of Figures

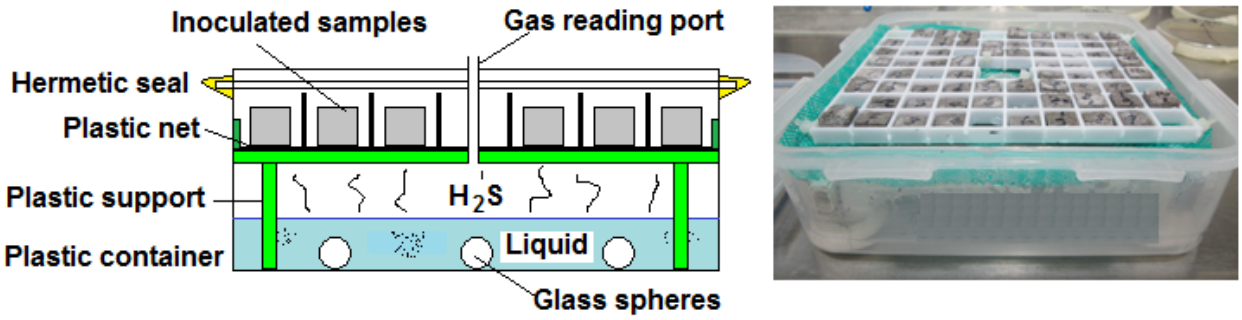

Fig. 1. Container used to maintain and expose mortar samples to hydrogen sulfide.

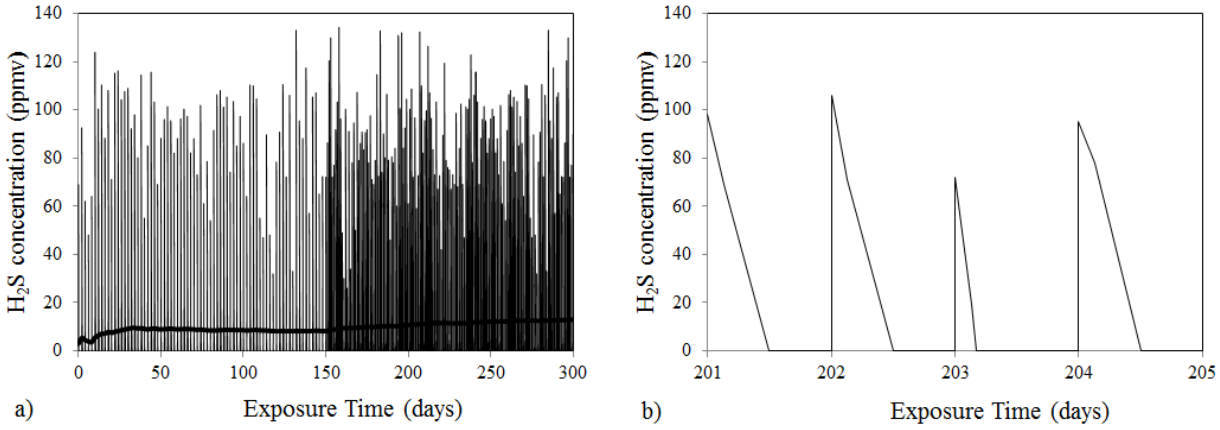

Fig. 2. Hydrogen sulfide concentration observed in one container: a) total time window (heavy line shows the continuous equivalent concentration), b) example of applications during 5 consecutive days.

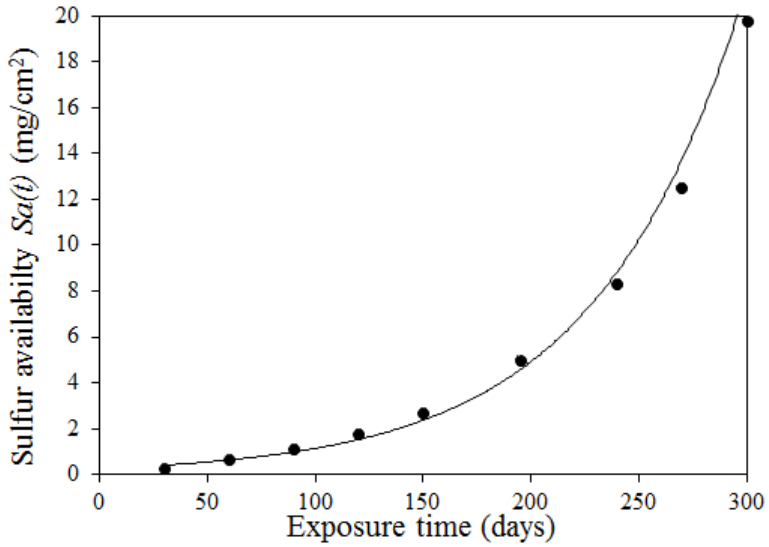

Fig. 3. Applied sulfur to exposed samples (sulfur availability).

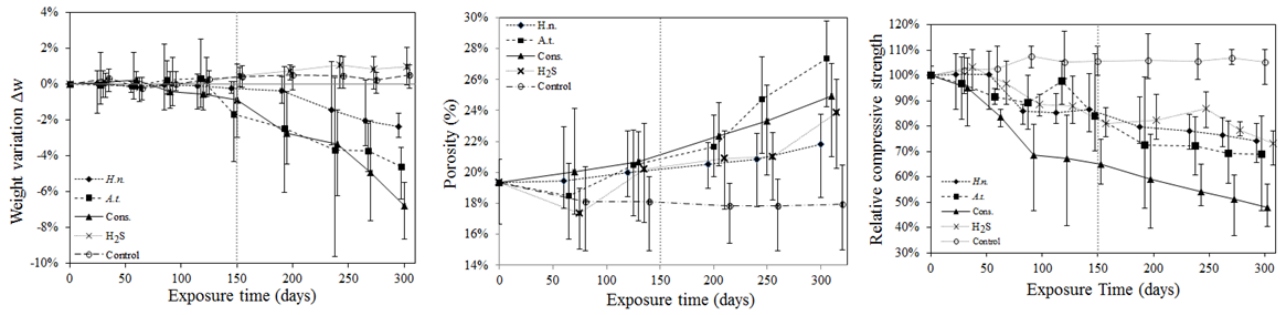

Fig. 4. Data from experiments for three studied effects variation (weight, porosity and strength).

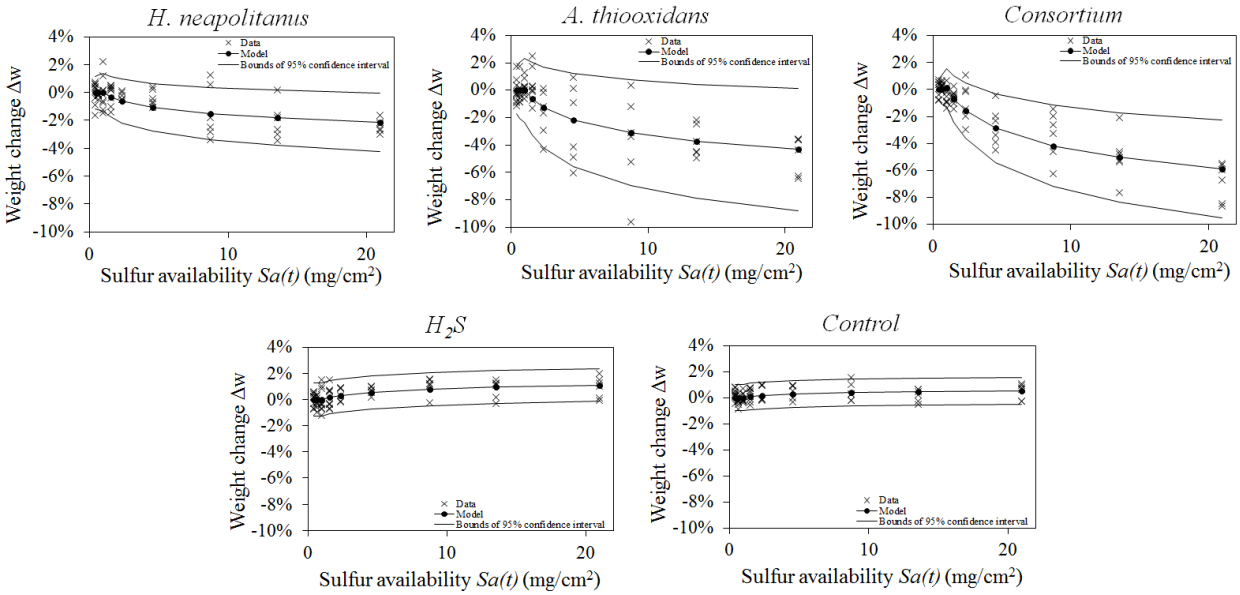

Fig. 5. Comparison between proposed models and measured data for weight change.

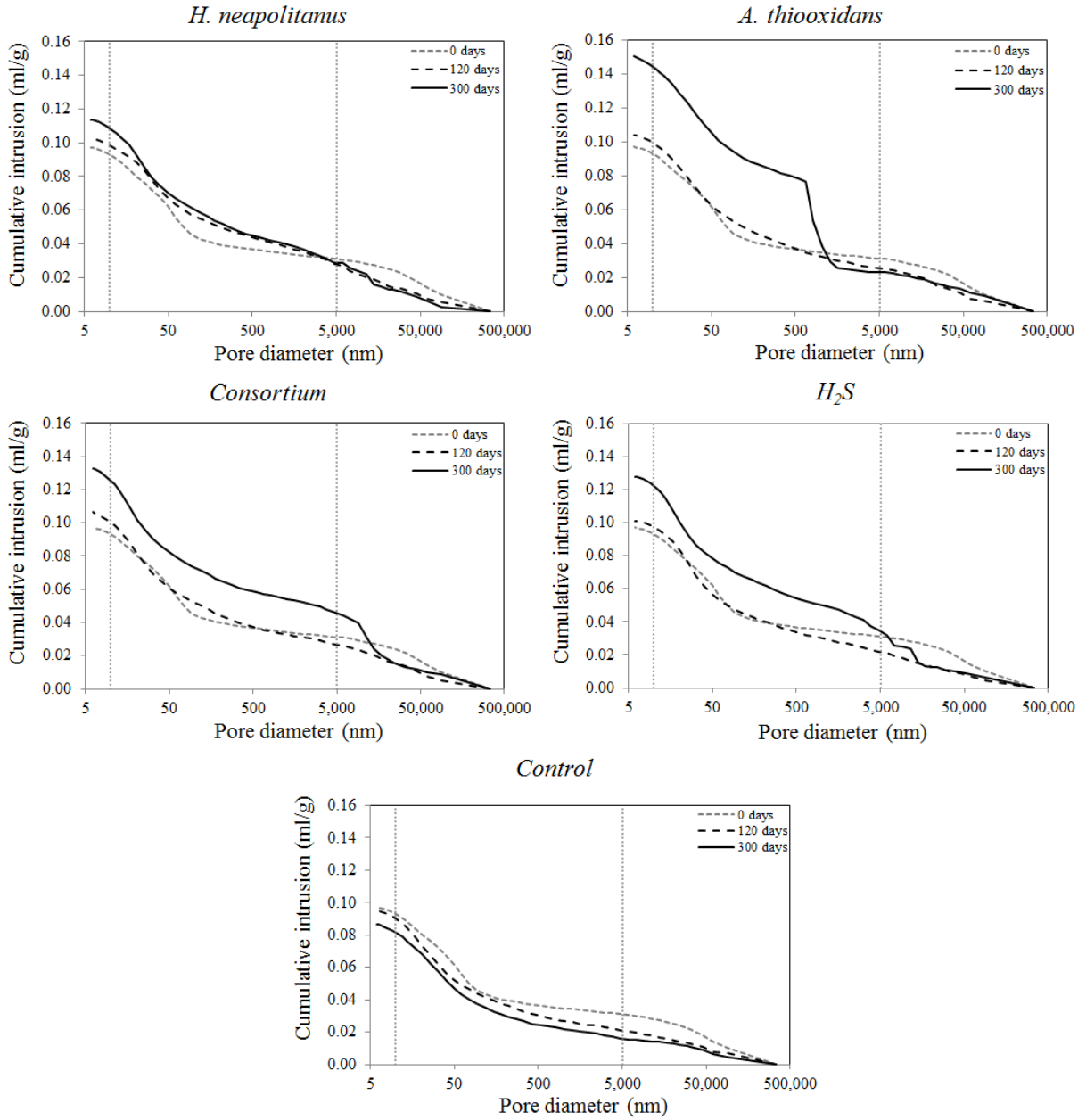

Fig. 6. Cumulative mercury intrusion versus pore size for all samples.

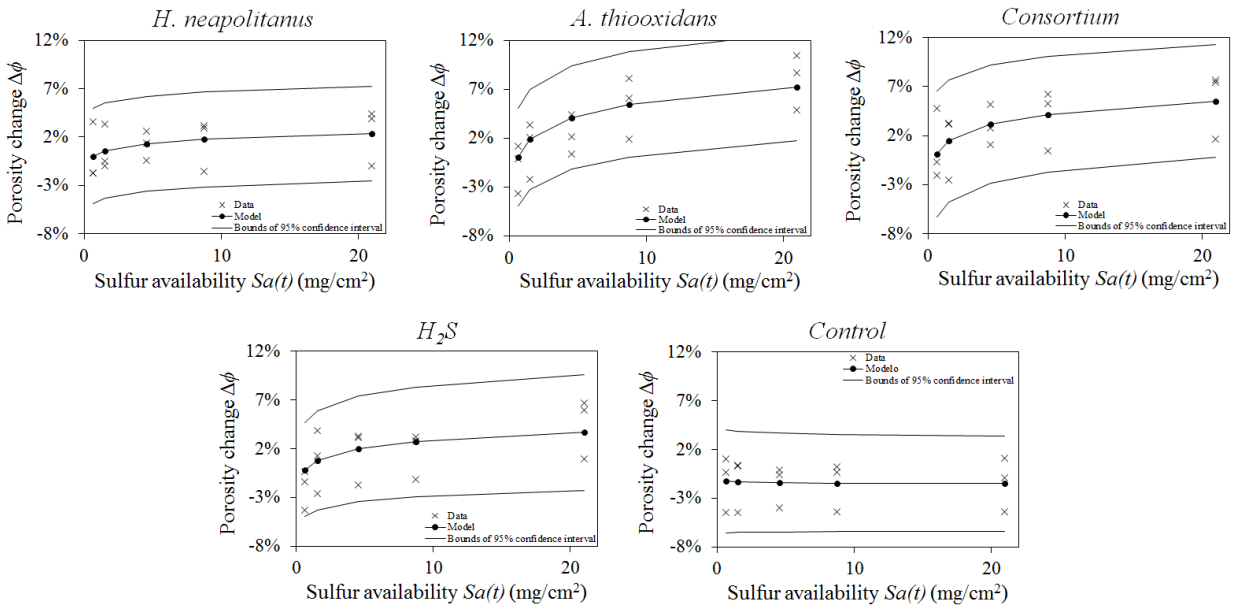

Fig. 7. Comparison between proposed models and measured data for porosity change.

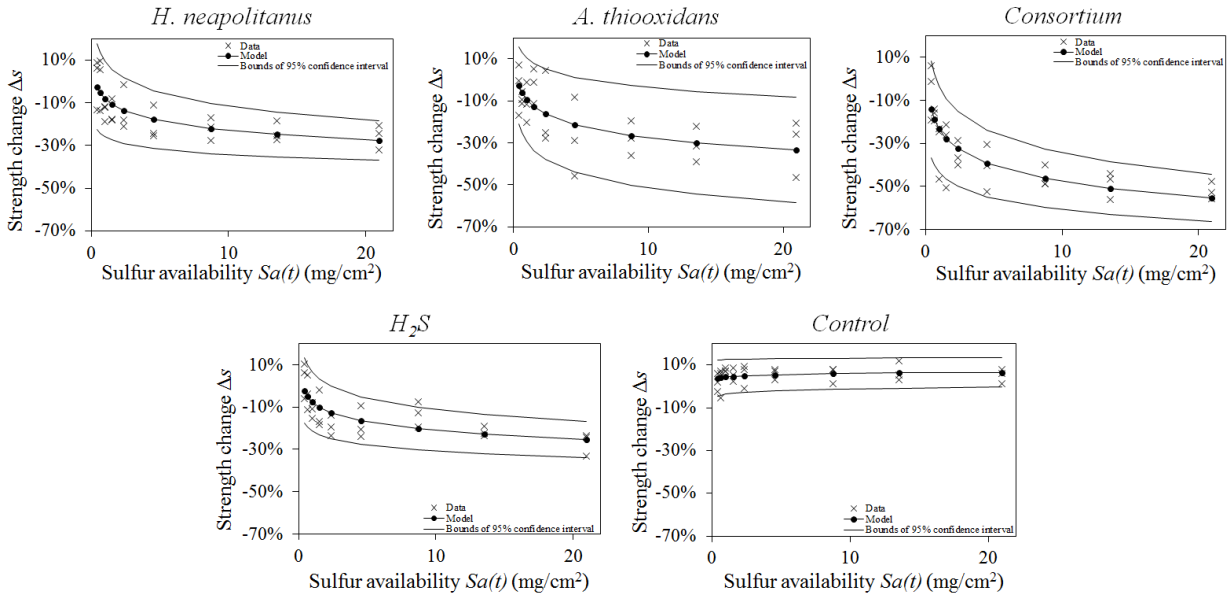

Fig. 8. Comparison between proposed models and measured data for strength change.

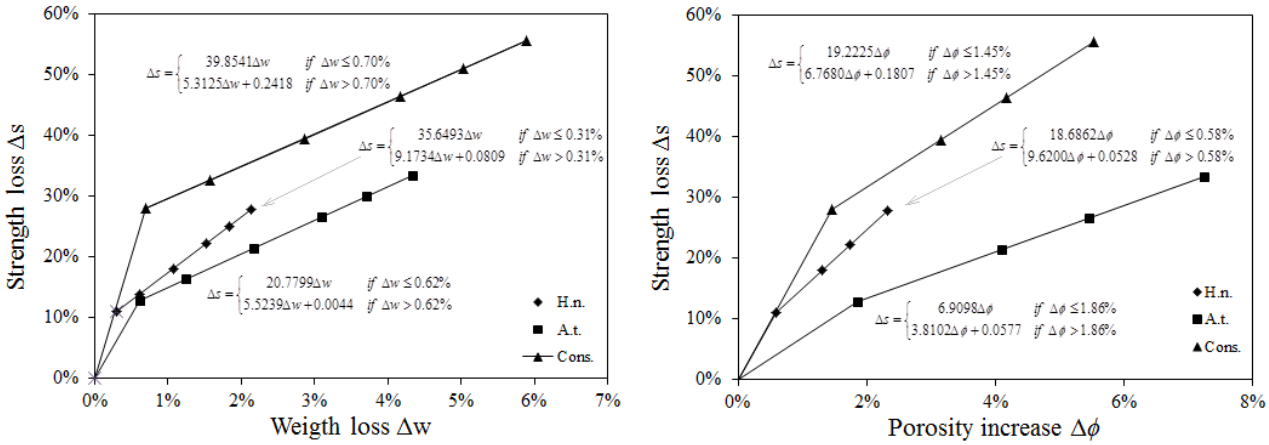

Fig. 9. Strength loss associated to porosity and weight changes in biodeteriorated samples.

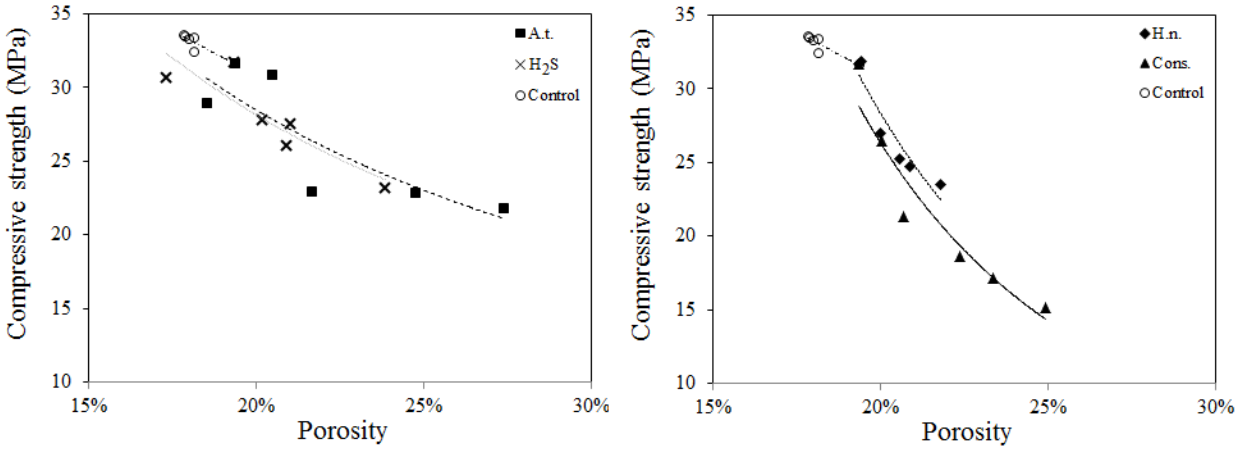

Fig. 10. Compressive strength to porosity relations associated to biodeterioration (this study).

List of tables

Table 1: Description of exposure environments.

Superficial treatment (inoculation)	Name	Feeding conditions
H. neapolitanus, standard medium	H.n.	100 ppmv H_2S, 0.3±0.1% CO_2
A. thiooxidans, standard medium	A.t.	100 ppmv H_2S, 0.3±0.1% CO_2
Consortium, standard medium	Cons.	100 ppmv H_2S, 0.3±0.1% CO_2
Chemical exposure (abiotic)	H_2S	100 ppmv H_2S, 0.3±0.1% CO_2
Control	Control	Ordinary humid atmosphere

Table 2: Initial and final porosities in pore ranges.

Pore size description	**Initial**	**Final (after 300 days of exposure)**				
		H. n.	***A. t.***	**Cons.**	**H_2S**	**Control**
Micro: 0-10 nm	1.1%	1.3%	1.5%	1.8%	1.4%	1.4%
Meso: 10-5000nm	12.1%	15.0%	21.7%	14.8%	16.6%	13.4%
Macro: >5000nm	6.1%	5.5%	4.2%	8.3%	5.9%	3.2%
Average Porosity	19.4%	21.8%	27.4%	24.9%	23.9%	18.0%

Table 3: Modeling of properties variation for $Sa(t) \geq 1$ mg/cm^2.

Experimental condition	Property variation	Standard deviation
Inoculated with *H.n.*	$\Delta w(Sa(t)) = -0.0070 \ln(Sa(t)) - 0.00020$	$\sigma_{ME,\Delta w}(Sa(t)) = 0.0012 \ln(Sa(t)) + 0.0070$
	$\Delta \phi(Sa(t)) = 0.0067 \ln(Sa(t)) + 0.0031$	$\sigma_{ME,\Delta \phi}(Sa(t)) = 0.022$
	$\Delta s(Sa(t)) = -0.064 \ln(Sa(t)) - 0.0823$	$\sigma_{ME,\Delta s}(Sa(t)) = 0.077$
Inoculated with *A.t.*	$\Delta w(Sa(t)) = -0.0140 \ln(Sa(t)) - 0.00030$	$\sigma_{ME,\Delta w}(Sa(t)) = 0.0035 \ln(Sa(t)) + 0.0120$
	$\Delta \phi(Sa(t)) = 0.0205 \ln(Sa(t)) + 0.0101$	$\sigma_{ME,\Delta \phi}(Sa(t)) = 0.025$
	$\Delta s(Sa(t)) = -0.078 \ln(Sa(t)) - 0.0961$	$\sigma_{ME,\Delta s}(Sa(t)) = 0.110$
Inoculated with Cons.	$\Delta w(Sa(t)) = -0.0200 \ln(Sa(t)) + 0.00120$	$\sigma_{ME,\Delta w}(Sa(t)) = 0.0037 \ln(Sa(t)) + 0.0073$
	$\Delta \phi(Sa(t)) = 0.0155 \ln(Sa(t)) + 0.0081$	$\sigma_{ME,\Delta \phi}(Sa(t)) = 0.027$
	$\Delta s(Sa(t)) = -0.105 \ln(Sa(t)) - 0.2353$	$\sigma_{ME,\Delta s}(Sa(t)) = 0.094$
Abiotic H_2S	$\Delta w(Sa(t)) = 0.0036 \ln(Sa(t)) + 0.00008$	$\sigma_{ME,\Delta w}(Sa(t)) = 0.0063$
	$\Delta \phi(Sa(t)) = 0.0109 \ln(Sa(t)) + 0.0034$	$\sigma_{ME,\Delta \phi}(Sa(t)) = 0.025$
	$\Delta s(Sa(t)) = -0.059 \ln(Sa(t)) - 0.0751$	$\sigma_{ME,\Delta s}(Sa(t)) = 0.069$
Control	$\Delta w(Sa(t)) = 0.0017 \ln(Sa(t)) + 0.00004$	$\sigma_{ME,\Delta w}(Sa(t)) = 0.0050$
	$\Delta \phi(Sa(t)) = -0.0007 \ln(Sa(t)) - 0.0130$	$\sigma_{ME,\Delta \phi}(Sa(t)) = 0.022$
	$\Delta s(Sa(t)) = 0.007 \ln(Sa(t)) + 0.0442$	$\sigma_{ME,\Delta s}(Sa(t)) = 0.038$